One-dimensional random Ising models

1985 J. Phys. A: Math. Gen. 18 621

(http://iopscience.iop.org/0305-4470/18/4/012)

J. Phys. A: Math. Gen. 18 (1985) 621-639. Printed in Great Britain

One-dimensional random Ising models

J M Normand, M L Mehta† and H Orland

Service de Physique Théorique, CEN Saclay, Orme des Merisiers, 91191 Gif-sur-Yvette, Cedex France

Received 11 June 1984

Abstract. A study of several one-dimensional random Ising chains and strips is presented. The free energy is expressed in terms of a probability distribution, the support of which is studied with use of a recurrence relation. The shape of the support is shown to vary from a connected set to a Cantor set depending on the type of randomness. Monte Carlo calculations and analytical approximations are presented.

1. Introduction

A lot of effort has been devoted to the study of disordered systems. In particular, the random bond or spin glass systems and the random field systems, although partly understood, remain rather mysterious. The difficulty in the study of these systems is that one has to make quenched averages, i.e. average observables or the free energy.

Several methods have been used in order to perform the quenched average, such as replicas (Edwards and Anderson 1975), the use of dynamics (De Dominicis 1978) and the averaging over stochastic equations of motion (De Dominicis 1979). However, none of these methods is really satisfactory, in the sense that at some stage some *ad hoc* ansatz has to be made in order to make the problem tractable.

The one-dimensional random-field Ising model has been solved for a specific type of randomness (Fan and McCoy 1969, Brandt and Gross 1978, Derrida *et al* 1978, Bruinsma and Aeppli 1983, Györgi and Rujoriginalán 1984) and exhibits a very rich behaviour with a transition line in the $(H/J, J/T)$ plane. These studies exhibit a devil's staircase integrated probability distribution. This behaviour is suggestive of the complexity that may occur in higher dimensions.

The previous results are generalised with respect to both the models and the nature of the randomness. We consider one-dimensional random-field Ising models as well as spin glass (i.e. random bond) models on a two-layer strip. These models are studied for various probability distributions of the random variables. In § 2, we present three simple spin Hamiltonians. The analytical relations between their partition functions are derived. The general formulation for the calculation of the free energy per site is given in § 3 assuming random couplings or fields. The result is given in terms of a probability density, the support of which is studied in § 4. Section 5 is devoted to some special cases which illustrate the results of § 4. In particular it is shown that under certain conditions the support undergoes a transition from a connected set to a Cantor set. Some numerical and analytical approximations are presented.

† Chercheur CNRS.

2. Three models and their interrelations

The three models we consider are:

(1) An Ising chain of N sites in a magnetic field (figure 1(a)). The Hamiltonian is for $N=2, 3, \ldots$

$$\mathscr{H}_N^1 = -\sum_{i=1}^{N-1} J_i\sigma_i\sigma_{i+1} - \sum_{i=1}^{N} H_i\sigma_i. \tag{2.1}$$

(2) An Ising strip of width two and $N/2-1$ squares (N sites, figure 1(b)). The Hamiltonian is for $N=4, 6, \ldots$

$$\mathscr{H}_N^S = -\sum_{i=1}^{N/2-1} (J_{1,i}\sigma_{1,i}\sigma_{1,i+1} + J_{3,i}\sigma_{2,i}\sigma_{2,i+1}) - \sum_{i=1}^{N/2} J_{2,i}\sigma_{1,i}\sigma_{2,i}. \tag{2.2}$$

(3) An Ising strip of width two and $t+t'$ triangles ($N=t+t'+2$ sites, figure 1(c)). The Hamiltonian is for $t=1, 2, \ldots$ and $t'=t-1$ or t

$$\mathscr{H}_N^T = -\sum_{i=1}^{t} J_{1,i}\sigma_{1,i}\sigma_{1,i+1} - \sum_{i=1}^{t'+1} J_{2,i}\sigma_{1,i}\sigma_{2,i} - \sum_{i=1}^{t'} J_{3,i}\sigma_{2,i}\sigma_{2,i+1} - \sum_{i=1}^{t} J_{4,i}\sigma_{1,i+1}\sigma_{2,i}. \tag{2.3}$$

Denoting by $\mathscr{H}$ these nearest neighbour (NN) Ising Hamiltonians, we consider the high-temperature expansion of the partition function for N sites

$$Z_N = \sum_{\{\sigma=\pm 1\}} \exp(-\beta\mathscr{H}), \tag{2.4}$$

which reads

$$Z_N = 2^N \prod_{\text{NN bonds}} \cosh(\beta J_{ss'}) \prod_{s=1}^{N} \cosh(\beta H_s) z_N, \tag{2.5}$$

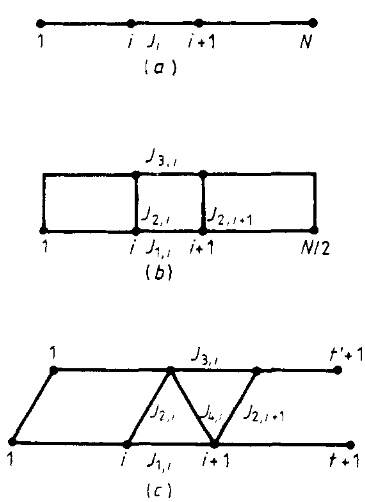

Figure 1. Labelling of coupling constants for the three Ising models considered.

where

$$z_N = \prod_{\text{NN bonds}} (1+x_{ss'}) \prod_{s=1}^{N} (1+h_s), \tag{2.6}$$

$$x_{ss'} = \tanh(\beta J_{ss'}), \qquad h_s = \tanh(\beta H_s), \tag{2.7}$$

and s and s' label the lattice sites.

We are interested in the free energy per site in the thermodynamic limit, i.e.

$$f = \lim_{N\to\infty} -(N\beta)^{-1} \ln Z_N, \tag{2.8}$$

the non-trivial part of which is given in terms of

$$g = \lim_{N\to\infty} g_N, \qquad g_N = N^{-1} \ln z_N. \tag{2.9}$$

We now derive a three-point recurrence relation for z_N which happens to be the same for the three systems considered. This recurrence relation is based on the graphical representation of the high-temperature expansion. Namely, z_N is expanded as a series of powers of $x_{ss'}$ and h_s and each term in the sum is represented by a configuration of paths drawn on the lattice. Each of these paths is either a closed polygon or a path with two ends, a bond being used at most once. For each path, each bond contributes an $x_{ss'}$ and each end point an h_s. In what follows, the x and the J related by equation (2.7) carry the same indices; these indices are specified in figure 1.

For the Ising chain in an external field, equation (2.5) reads

$$Z_N^1 = 2^N \prod_{i=1}^{N-1} \cosh(\beta J_i) \prod_{i=1}^{N} \cosh(\beta H_i) z_N^1. \tag{2.10}$$

On a chain there is no closed polygon and only paths with two end points contribute to z_N^1. Thus z_{N+1}^1 is a sum of three terms

$$z_{N+1}^1 = z_N^1 + z_{N-1}^1 x_N h_N h_{N+1} + (z_N^1 - z_{N-1}^1) x_N h_{N+1}/h_N, \tag{2.11}$$

which correspond respectively to all configurations of paths (i) without the bond N, $N+1$, (ii) without the bond $N-1$, N but with the bond N, $N+1$ and (iii) with both the bonds $N-1$, N and N, $N+1$. Ignoring the upper index of z, the initial conditions are

$$z_0 = z_1 = 1. \tag{2.12}$$

For a strip of squares, labelling z by $n = \frac{1}{2}N$, one has

$$Z_N^S = 2^N \cosh \beta J_{2,n} \prod_{\alpha=1}^{3} \prod_{i=1}^{n-1} \cosh(\beta J_{\alpha,i}) \cdot z_n^S. \tag{2.13}$$

In zero field, only closed polygons contribute to z_n^S. Arguments similar to the above give

$$z_{n+1}^S = z_n^S + z_{n-1}^S x_{1,n} x_{2,n} x_{3,n} x_{2,n+1} + (z_n^s - z_{n-1}^s) x_{1,n} x_{3,n} x_{2,n+1}/x_{2,n}, \tag{2.14}$$

with the initial conditions (2.12).

For a strip of triangles, labelling z by $n = N-1$, one has

$$Z_N^T = 2^N \prod_{\text{NN bonds}} \cosh(\beta J_{ss'}) z_n^T, \tag{2.15}$$

where z_n^{T} satisfies equation (2.12) and a three-point recurrence relation similar to equation (2.14).

Hence, in these three cases the recurrence relation for z is of the form

$$z_{n+1}=(1+a_n)z_n-a_n(1-b_n)z_{n-1}, \qquad n=1,2,\ldots \tag{2.16}$$

with the initial conditions (2.12). The a_n and b_n are listed in table 1 and satisfy

$$0\leqslant b_n\leqslant 1, \qquad 0\leqslant a_n^2 b_n/b_{n+1}\leqslant 1, \qquad n=1,2,\ldots. \tag{2.17}$$

If one has the same set $\{a_n;\ n=1,2,\ldots\}$ and the same set $\{b_n;\ n=1,2,\ldots\}$ for any two of the three cases considered above, the recurrence relations (2.16) will be the same. The initial conditions being the same, the corresponding z_n will be equal. One thereby relates the partition functions Z_n^{I}, Z_{2n}^{S} and Z_{n+1}^{T}, i.e. they differ only by powers of two and products of factors cosh βJ and cosh βH. This equivalence between the three cases can also be obtained directly by suitable changes of the variables σ_s in (2.4)†.

Let us notice that a recurrence relation similar to equation (2.16) can also be derived for the O(n) vector spin model for the square strip problem. This study will be published elsewhere.

3. General formulation for random systems

In the models of disordered systems the coefficients of the recurrence relation for z_N are random variables. Then the calculation of g is seen to be equivalent to finding the behaviour for large N of a product of either N two by two random matrices or N random homographic transformations. It is also equivalent to solving an integral equation for a probability density $P(r)$ such that

$$g=\int \mathrm{d}r\ P(r)\ln(1+r). \tag{3.1}$$

The quantity g is usually referred as the Lyapunov exponent of the probability density.

Indeed, to go further in the computation of z_n, let u_i, v_i be defined by

$$\begin{pmatrix} u_{i+1}\\ v_{i+1}\end{pmatrix}=M_i\begin{pmatrix} u_i\\ v_i\end{pmatrix}, \qquad M_i=\begin{pmatrix} 1+a_i & -a_i(1-b_i)\\ 1 & 0\end{pmatrix}, \qquad i=1,2,\ldots \tag{3.2}$$

with $u_1=v_1=1$. Then one has

$$z_n=u_n, \qquad n=1,2,\ldots. \tag{3.3}$$

Another formulation in terms of homographic mappings is obtained by setting $u_i/v_i=1+r_i$, $i=1,2,\ldots$. Then one gets $r_1=0$ and

$$r_{i+1}=a_i(r_i+b_i)/(r_i+1)=T_i(r_i), \qquad i=1,2,\ldots. \tag{3.4}$$

Instead of T_i we also use the notation T_{a_i,b_i}. Equation (3.3) now becomes

$$z_n=\prod_{i=1}^{n}(1+r_i). \tag{3.5}$$

† We are grateful to B Derrida for informing us that the similarity between Z_n^{I} and Z_{2n}^{S} was also noticed by Maillard (1978).

Let the a_i and b_i take values which are either well defined or at random with a normalised probability density $p_n(a_n, b_n; \ldots; a_1, b_1)$. It follows that the normalised density distribution $P_n(r)$ of the r is given for $n = 1, 2, \ldots$ by

$$P_n(r) = \int \prod_{i=1}^{n} \mathrm{d}a_i \, \mathrm{d}b_i \, p_n(a_n, b_n; \ldots; a_1, b_1) \delta[r - T_n \ldots T_1(0)], \tag{3.6}$$

and the integrated distribution function $F_n(r)$ reads

$$F_n(r) = \int_{-\infty}^{r} \mathrm{d}r' \, P_n(r')$$
$$= \int \prod_{i=1}^{n} \mathrm{d}a_i \, \mathrm{d}b_i p_n(a_n, b_n; \ldots; a_1, b_1) \theta[r - T_n \ldots T_1(0)]. \tag{3.7}$$

As the partition function (2.4) is positive, so is z_n. Hence $1 + r_i$ is positive for $i = 1, 2, \ldots$. Therefore, $P_n(r)$ and $F_n(r)$ vanish for $r < -1$. Then the non-trivial part g_N, equation (2.9), of the free energy per site is expressed in terms of

$$\frac{1}{n} \ln z_n = \frac{1}{n} \sum_{i=1}^{n} \ln(1 + r_i) = \int \mathrm{d}r \, P_n(r) \ln(1 + r). \tag{3.8}$$

In order to obtain the thermodynamic limit (2.8) one has to find the behaviour for large n of either the product of matrices $M_n \ldots M_1$ or the density distribution $P_n(r)$. Assuming the pairs a_i, b_i independent and distributed according to $p(a_i, b_i)$ and taking the limit of $P_n(r)$ as n goes to infinity, one gets a stationary distribution $P(r)$; solution of the integral equation (Dyson 1953)

$$P(r) = \int \mathrm{d}a \, \mathrm{d}b \, p(a, b) \int \mathrm{d}r' \, P(r') \delta\{r - T_{a,b}(r')\}, \tag{3.9}$$

with the boundary condition

$$P(r) = 0 \qquad \text{for} \qquad r < -1. \tag{3.10}$$

Then g is given by (3.1). The integrated distribution function satisfies (provided $T_{a,b}$ has an inverse $T_{a,b}^{-1}$, i.e. $a \neq 0$)

$$F(r) = \int \mathrm{d}a \, \mathrm{d}b \, p(a, b) \{\theta(r - a) + \mathrm{sgn}(a) F[T_{a,b}^{-1}(r)]\}, \tag{3.11}$$

where $\mathrm{sgn}(a) = 1$ if $a > 0$ and -1 if $a < 0$, and $F(r)$ vanishes for $r < -1$.

For the existence of the thermodynamic limit g and the stationary distribution $P(r)$ referred above, we can appeal to Furstenberg's theorems (Furstenberg 1963). Actually Furstenberg's results do not always apply as such. Indeed, the matrix elements of M_i may be negative and furthermore these matrices are not always independent. This follows from the fact that it is the $J_{ss'}$ and H_s which are assumed to be either well defined or independent random variables. Then, from the relations given in table 1, if the b_i are still independent, this may no longer be true for the a_i. Indeed, a_i depends upon the ratio of parameters at two different sites. For example, if the H_i and thus the h_i, $i = 1, \ldots, n$ are independent random variables with the same probability density $\mu(h_i)$, one sees that for $n = 2, 3, \ldots$ the ratios $\rho_i = h_{i+1}/h_i$, $i = 1, \ldots, n-1$ are distributed

Table 1. Parameters a_i and b_i for the three systems considered. N is the number of sites.

$i=1,\ldots,n-1$	Chain $n=N$	Square strip $n=N/2$	Triangular strip $n=N-1=t+t'+1$	
			$i=2p-1=1,3,\ldots$	$i=2p=2,4,\ldots$
a_i	$x_i\dfrac{h_{i+1}}{h_i}$	$x_{1,i}, x_{3,i}\dfrac{x_{2,i+1}}{x_{2,i}}$	$x_{1,p}\dfrac{x_{4,p}}{x_{2,p}}$	$x_{3,p}\dfrac{x_{2,p+1}}{x_{4,p}}$
b_i	h_i^2	$(x_{2,i})^2$	$(x_{2,p})^2$	$(x_{4,p})^2$

with a probability density

$$P(\rho_1,\ldots,\rho_{n-1})=\int_{-\infty}^{+\infty}\mathrm{d}h\, h^{n-1}|\rho_1^{n-2}\rho_2^{n-3}\ldots\rho_{n-2}|\mu(h)\mu(\rho_1 h)\ldots\mu(\rho_{n-1}\ldots\rho_1 h). \tag{3.12}$$

Hence, the ρ_i are not independent, except if the density $\mu(h)$ is uniform. The qualitative relations between the parameters $J_{ss'}$, H_s and a_i, b_i are summarised in table 2.

Table 2. Qualitative relations between the parameters $J_{ss'}$, H_s and a_i, b_i for the Ising chain and the square strip. For physical cases, a_i and b_j must satisfy equation (2.17).

Ising	Square strip	a_i		$0\leqslant b_i\leqslant 1$
$H_i=H$ J_i random	$J_{2,i}=J_2$ $J_{1,i}$ and (or) $J_{3,i}$ random	random, independent	$\lvert a_i\rvert\leqslant 1$	b
$H_i=\begin{cases}H & \text{prob.}\\ -H & \text{prob. } 1-p\end{cases}$	$J_{2,i}=\begin{cases}J_2 & \text{prob. } p\\ -J_2 & \text{prob. } 1-p\end{cases}$	random, not independent	except if $p=\frac{1}{2}$	
H_i random ($\neq\pm H$) J_i random	$J_{2,i}$ random ($\neq\pm J_2$) $J_{1,i}$ and (or) $J_{3,i}$ random	random, not independent except if the distribution of H_i (or $J_{2,i}$) is uniform		random, independent

Nevertheless, Furstenberg's results apply to a product of transfer matrices in terms of which the partition function (2.4) can be expressed thereby proving the existence of f.

From now on we consider for simplicity only the cases when b_i takes a fixed value $b(0\leqslant b\leqslant 1)$ and the $a_i(|a_i|\leqslant 1)$ are independent random variables with a probability density $p(a)$. As we are unable to solve the integral equations (3.9) or (3.11), we study the support $\mathcal{S}$ of the probability density $P(r)$ through the iteration equation (3.4). General properties of $\mathcal{S}$ are derived in § 4 and they are illustrated for some particular cases in § 5.

4. General properties of the support of $P(r)$

All the results we derive for $\mathcal{S}$ are based on the following properties of the mapping $T_a(r)\equiv T_{a,b}(r)$ (from now on we will drop the fixed index b), see figure 2:

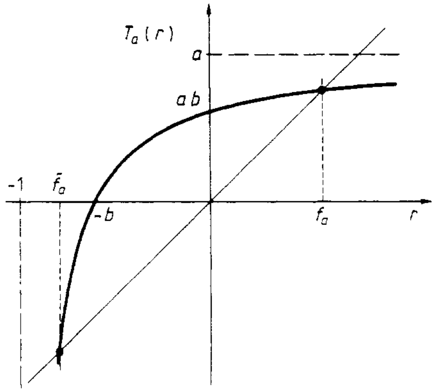

Figure 2. $T_a(r)$ with $a > 0$. The stable and unstable fixed points are respectively f_a and $\tilde{f}_a$.

(i) $T_a(r)$ is a monotonous increasing (resp. decreasing) function of r when a is positive (resp. negative).

(ii) It is a monotonous increasing function of a.

(iii) It has two real fixed points. Actually, we use the homographic character of T_a only to compute these points:

$$f_a = \tfrac{1}{2}(a - 1 + \Delta^{1/2}), \qquad \tilde{f}_a = \tfrac{1}{2}(a - 1 - \Delta^{1/2})$$
$$\Delta = (1-a)^2 + 4ab = (1+a)^2 - 4a(1-b), \tag{4.1}$$

and f_a is stable while $\tilde{f}_a$ is unstable. Furthermore (3.4) can be rewritten as

$$\frac{r_{i+1} - f_a}{r_{i+1} - \tilde{f}_a} = k_a \frac{r_i - f_a}{r_i - \tilde{f}_a}, \qquad k_a = \frac{1 + a - \Delta^{1/2}}{1 + a + \Delta^{1/2}}, \tag{4.2}$$

and k_a has the same sign as a. Hence for large i, r_i tends to f_a either in a monotonous or oscillating way according to whether a is positive or negative.

(iv) $T_a(r)$ is linear in a and $T_{-a}(r) = -T_a(r)$.

(v) For all $a \neq 0$, $T_a(r)$ maps the real line $\mathbb{R}$ onto itself.

Let $\mathscr{A}$ be the set of possible values of a. From equation (3.6) the support $\mathscr{S}_n$ of $P_n(r)$ is

$$\mathscr{S}_n = \{T_{a_n} \ldots T_{a_1}(0);\ \forall a_n, \ldots, a_1 \in \mathscr{A}\}, \tag{4.3}$$

namely a set of at most $\mathscr{N}^n$ points if $\mathscr{A}$ has a finite number $\mathscr{N}$ of elements. If zero is a possible value of a, then, since $T_0(r) = 0$, one generates at each step of iteration the initial value $r = 0$. One therefore has

$$\text{if} \qquad 0 \in \mathscr{A} \qquad \text{then} \qquad \mathscr{S}_n \subseteq \mathscr{S}_{n+1}, \qquad n = 0, 1, \ldots. \tag{4.4}$$

It follows from property (iv) and equation (3.6) that

$$\text{if} \qquad p(a) = p(-a) \qquad \text{then} \qquad P(r) = P(-r), \tag{4.5}$$

and therefore also $F(r) + F(-r) = 1$.

Using the iterative scheme, we determine in appendix 1 the minimum and the maximum values $r_{\min}$ and $r_{\max}$ that r takes in the support $\mathscr{S}$. These values are listed

Table 3. r_{min} and r_{max} are the end points of the smallest interval $\mathscr{R}_0$ outside of which $P(r)$ vanishes. The maximum and the minimum values taken by the parameter a are given in terms of the α in the first column for the three considered cases, cf appendix 1. f_α is the attractive fixed point of T_α gaven by equation (4.1).

$\mathscr{A}$	r_{min}	r_{max}
$0 \leq \alpha_{min} \leq \alpha_{max} \leq 1$	$f_{\alpha_{min}}$	$f_{\alpha_{max}}$
$-1 \leq \tilde{\alpha}_{min} \leq \tilde{\alpha}_{max} \leq 0$ $0 \leq \alpha_{min} \leq \alpha_{max} \leq 1$	$T_{\tilde{\alpha}_{min}}(f_{\alpha_{min}})$	$f_{\alpha\, max}$
$-1 \leq \tilde{\alpha}_{min} \leq \tilde{\alpha}_{max} \leq 0$	attractive fixed point of $T_{\tilde{\alpha}_{min}} T_{\tilde{\alpha}_{max}}$	attractive fixed point of $T_{\tilde{\alpha}_{max}} T_{\tilde{\alpha}_{min}}$

in table 3 for the three cases we have to distinguish namely a takes values which are (1) non-negative, (2) positive and negative and (3) non-positive. Hence the support $\mathscr{S}$ of $P(r)$ is within the finite interval $\mathscr{R}_0$

$$\mathscr{S} \subseteq \mathscr{R}_0 = [r_{min}, r_{max}], \tag{4.6}$$

and $P(r)$ vanishes outside $\mathscr{R}_0$, i.e. on

$$\mathscr{D}_0 = \mathbb{R} - \mathscr{R}_0, \tag{4.7}$$

The interval $\mathscr{R}_0$ is also characterised by the following property: it is the largest interval such that

$$\forall r \in \mathscr{R}_0 \qquad \text{and} \qquad \forall a \in \mathscr{A} \qquad T_a(r) \in \mathscr{R}_0. \tag{4.8}$$

In other words, once a point r belongs to $\mathscr{R}_0$, all its images in the iterative procedure remain in $\mathscr{R}_0$. This follows from the property (iii) and the attractive character of the fixed points in terms of which r_{min} and r_{max} are defined.

Now, since $P(r)$ vanishes on $\mathscr{D}_0$, from equation (3.9) it also vanishes on the intersection of the images $T_a(\mathscr{D}_0)$ for all a in $\mathscr{A}$. Repeating this argument one finds that $P(r)$ vanishes on

$$\mathscr{D}_{i+1} = \bigcap_{a \in \mathscr{A}} T_a(\mathscr{D}_i), \qquad i = 0, 1, \ldots. \tag{4.9}$$

Consequently, the support $\mathscr{S}$ of $P(r)$ is within the complement of $\mathscr{D}_i$ with respect to the real line, i.e.

$$\mathscr{S} \subseteq \mathscr{R}_i = \mathbb{R} - \mathscr{D}_i, \qquad i = 0, 1, \ldots. \tag{4.10}$$

It is shown in appendix 2 that the sequence of the sets $\mathscr{R}_i$ is also defined by

$$\mathscr{R}_{i+1} = \bigcup_{a \in \mathscr{A}} T_a(\mathscr{R}_i), \qquad i = 0, 1, \ldots. \tag{4.11}$$

and furthermore it forms a sequence of nested intervals

$$\mathscr{R}_{i+1} \subseteq \mathscr{R}_i, \qquad i = 0, 1, \ldots \tag{4.12}$$

or equivalently from (4.10) $\mathscr{D}_i \subseteq \mathscr{D}_{i+1}$. Depending upon the set $\mathscr{A}$ and the value b it is possible that $\mathscr{R}_1 = \mathscr{R}_0$ or that $\mathscr{R}_{i+1} = \mathscr{R}_i$ from some i onwards. Then $\mathscr{S} = \mathscr{R}_i$. On the other hand if $\mathscr{R}_{i+1}$ is strictly included in $\mathscr{R}_i$ for any i, then at each step a new domain

$\mathcal{R}_i - \mathcal{R}_{i+1}$ is excluded from the support $\mathcal{S}$. In other words, more and more 'holes' appear in $\mathcal{R}_0$ and the support of $P(r)$ may reduce to a Cantor set, cf § 5.1.

It should be noted that all the previous discussion of the support of $P(r)$ depends only upon the value of b and the support $\mathcal{A}$ of $p(a)$, but not upon the value of the probability density $p(a)$ itself. All these general considerations are now illustrated with some particular examples.

5. Some special cases

The support of $P(r)$ is studied in the case where the a_i take firstly only two values and then more than two values. We end this section with some results about the integrated distribution function. Typical cases are illustrated by numerical examples. The distribution $P(r)$ is computed by the Monte Carlo method: the a_i are sampled according to $p(a)$ and the recurrence relation (3.4) is iterated throwing away the first generations of points.

5.1. *The a_i take only two values*

(i) Let us denote these values by γ_1 and γ_2. For brevity, we note $T_i \equiv T_{\gamma_i}$ and the attractive fixed point $f_i = f_{\gamma_i}$; $i = 1, 2$, given by equation (4.1). The three cases we have to distinguish are

(1) $0 \leq \gamma_1 < \gamma_2 \leq 1$,
(2) $-1 \leq \gamma_1 < 0 \leq \gamma_2 \leq 1$,
(3) $-1 \leq \gamma_1 < \gamma_2 \leq 0$.

They are associated with figures 3, 4 and 5 respectively. The support $\mathcal{S}$ of $P(r)$ is such that $\mathcal{S} \subseteq \mathcal{R}_0 = [r_{\min}, r_{\max}]$. The values of $r_{\min}$ and $r_{\max}$ are given on the corresponding figures, except for the third case where the expressions are more complicated, cf table 3. From equation (4.11) $\mathcal{R}_1 = T_{\gamma_1}(\mathcal{R}_0) \cup T_{\gamma_2}(\mathcal{R}_0)$, and two cases may occur:

(1) $\mathcal{R}_1 = \mathcal{R}_0$ (figures 3(a), 4(a) and 5(a)) then the support of $P(r)$ is $\mathcal{S} = \mathcal{R}_0$.

(2) $\mathcal{R}_1 \subset \mathcal{R}_0$ (figures 3(b), 4(b) and 5(b)), then a first hole $\mathcal{H}_1 = \mathcal{R}_0 - \mathcal{R}_1$ excluded from $\mathcal{S}$ appears in $\mathcal{R}_0$. This happens iff

(1) $T_1(r_{\max}) < T_2(r_{\min})$,
(2) $T_1(r_{\min}) < T_2(r_{\min})$,
(3) $T_1(r_{\min}) < T_2(r_{\max})$,

respectively for the three cases considered. In appendix 3 we discuss in terms of γ_1, γ_2 and b when the two previous conditions can be realised, see also figure 6. Now if $\mathcal{H}_1$ is not empty, it is easy to show on the figures, but cumbersome to describe, that $\mathcal{R}_2 = \mathcal{R}_1 - \mathcal{H}_2$ where the new domain $\mathcal{H}_2$ excluded from $\mathcal{S}$ is the direct sum of $T_1(\mathcal{H}_1)$ and $T_2(\mathcal{H}_1)$. Repeating this argument, one finds that all the images of $\mathcal{H}_1$ obtained by applying T_1 or T_2 any number of times and in any order are pairwise disjoint and thus excluded from $\mathcal{S}$. These results directly follow from the fact that $T_a(r)$ is a monotonous function of r. Thus the number of holes has the power of the continuum. The support $\mathcal{S}$ contains the end points of these holes, hence it has also the power of the continuum. Actually $\mathcal{S}$ consists of the fixed points of any finite sequence of T_i, their images and their accumulation points. Consequently in every neighbourhood of a point of $\mathcal{S}$ there

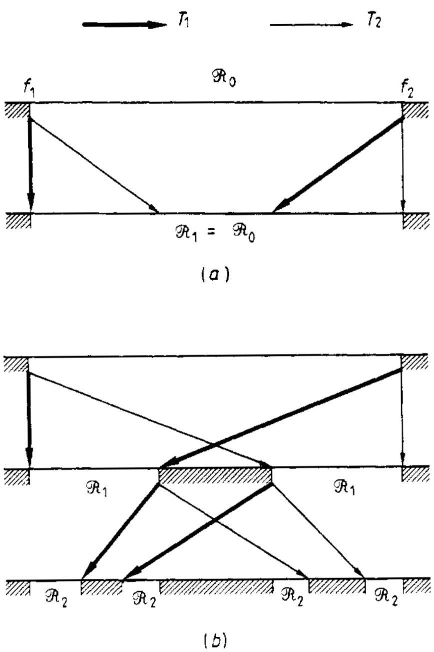

Figure 3. The mappings T_i and the first intervals $\mathcal{R}_j$. The a_i take two positive values γ_1 and γ_2. In (*a*) the support of $P(r)$ is $\mathcal{S} = \mathcal{R}_0$ and in (*b*) there exists an infinite number of holes in $\mathcal{R}_0$.

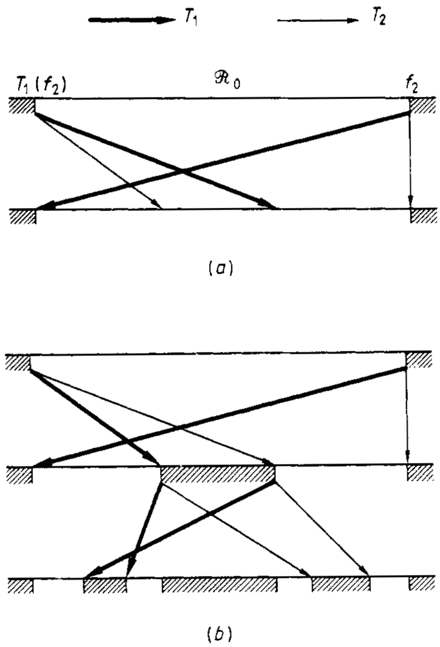

Figure 4. The same as in figure 3, except that now the values of a_i are $\gamma_1 < 0$ and $\gamma_2 > 0$.

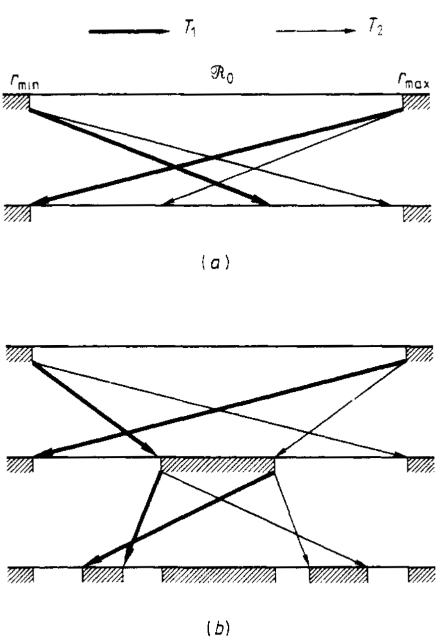

Figure 5. The same as in figure 3, except that now the values of a_i are $\gamma_1 < \gamma_2 < 0$.

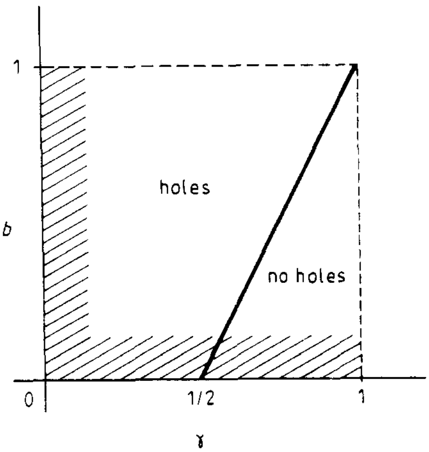

Figure 6. The γb plane when the a_i take two values $+\gamma$ and $-\gamma$. According to equation (A3.4) the critical line is indicated. The approximation studied in § 5.1. (ii) is valid in the hatched region.

is a hole. The support $\mathscr{S}$ of $P(r)$ is then a Cantor set (e.g. Hausdorff 1957). Figures 7 and 8 show Monte Carlo calculation for some typical cases.

(ii) To illustrate the previous results we give an analytical approximation in the case when the a_i take the values $\pm a$ $(a > 0)$ with probability $\frac{1}{2}$. Let us define

$$b^{1/2} = \tanh \varphi,$$
$$r_n = b^{1/2} \tanh \theta_n, \tag{5.1}$$
$$f = \tfrac{1}{2}\{-(1-a) + [(1-a)^2 + 4ab]^{1/2}\} = b^{1/2} \tanh \theta^*.$$

The recurrence relation (3.4) becomes

$$\tanh \theta_{n+1} = \varepsilon_n a \tanh(\theta_n + \varphi), \tag{5.2}$$

where ε_n is ± 1 with probability $\frac{1}{2}$. Two cases can be approximated easily:

(1) $a \to 0$, then θ_n is of order a and the equation (5.2) can be expanded as

$$\theta_{n+1} = \varepsilon_n a[b^{1/2} + \theta_n(1-b)]. \tag{5.3}$$

(2) $b \to 0$ and $a \neq 1$, then $f \sim [a/(1-a)]\, b$ and thus $\theta^* \sim [a/(1-a)]\, b^{1/2}$. Since φ is of order $b^{1/2}$ and $|\theta_n| \leq \theta^*$, θ_n is also of order $b^{1/2}$ and equation (5.2) becomes

$$\theta_{n+1} = \varepsilon_n a(b^{1/2} + \theta_n). \tag{5.4}$$

Both equations (5.3) and (5.4) are of the same type, and their solutions read

$$\theta_n = ab^{1/2}(\varepsilon_{n-1} + \varepsilon_{n-1}\varepsilon_{n-2}\lambda + \ldots + \varepsilon_{n-1} \ldots \varepsilon_1 \lambda^{n-2}), \tag{5.5}$$

where in case (1) $\lambda = a(1-b)$ and in case (2) $\lambda = a$. Since the ε_i are independent random variables equal to ± 1 with probability $\frac{1}{2}$, the same holds true for any of their products. Therefore the last equation takes the form

$$\theta_n = ab^{1/2} \sum_{p=1}^{n-1} \varepsilon_p \lambda^{p-1}. \tag{5.6}$$

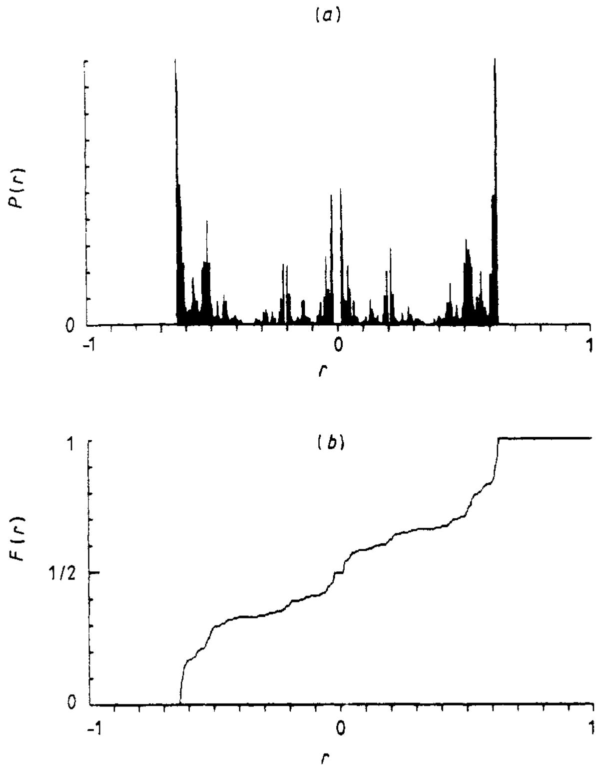

Figure 7. (a) The probability distribution $P(r)$ and (b) the integrated probability distribution $F(r)$, calculated with 11 000 iterations, discarding the first 1000. Figure (a) is a histogram with 640 bins on the r axis. The parameters are $\gamma_2 = -\gamma_1 = 0.81$ and $b = 0.64$. The support of $P(r)$ is a Cantor set, and $F(r)$ is a devil's staircase.

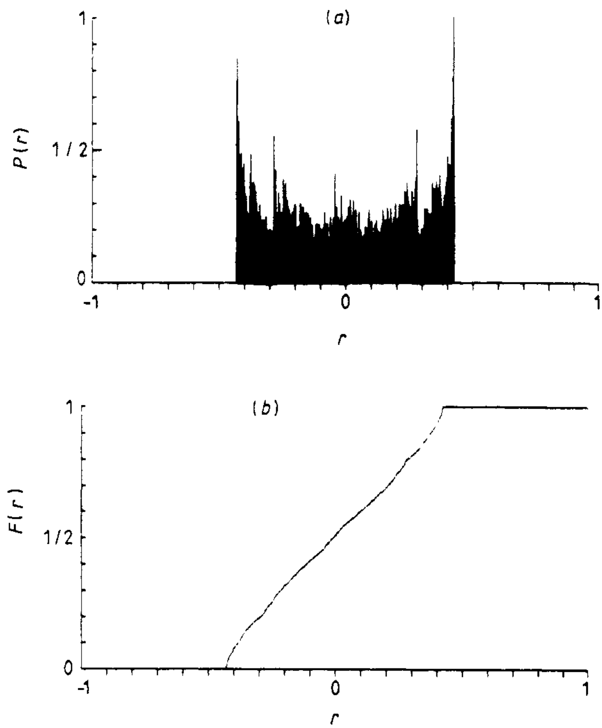

Figure 8. Same as figure 7. The parameters are $\gamma_2 = -\gamma_1 = 0.9$ and $b = 0.25$. The support of $P(r)$ is connected and $F(r)$ is continuous.

Now, setting $\varepsilon_p = 2n_p - 1$, the n_p are independent random variables equal to 0 or 1 with probability $\frac{1}{2}$, and the above equation becomes

$$\theta_n = ab^{1/2}\left(2\sum_{p=1}^{n-1} n_p\lambda^{p-1} - \frac{\lambda_n - 1}{\lambda - 1}\right). \tag{5.7}$$

Since we are interested in the tail of the distribution of the θ_n and $\lambda < 1$, equation (5.7) simplifies to

$$\theta_n = 2ab^{1/2}\sum_{p=1}^{n-1} n_p\lambda^{p-1} - \frac{ab^{1/2}}{1-\lambda}. \tag{5.8}$$

It follows that the support of the θ_n is either a Cantor set if $\lambda < \frac{1}{2}$ or a connected segment if $\lambda \geq \frac{1}{2}$. Thus in case (1), since $\lambda \to 0$ the support is always a Cantor set, whereas in case (2) the support exhibits a transition for $a = \frac{1}{2}$ which is on the transition line $2a = 1 + b$, equation (A3.4), in the limit $b \to 0$, see figure 6.

The Lyapunov exponent, equation (3.1), can be computed in this approximation. One finds

$$g = -\tfrac{1}{2}a^2b^2(1-\lambda^2)^{-1}. \tag{5.9}$$

As expected in a one-dimensional system, the free energy, related to g by equations (2.8) and (2.9) does not have any singularity.

5.2. The a_i take more than two discrete values

The description of the support $\mathcal{S}$ of $P(r)$ can now be more complicated. We illustrate this by describing the generic case where the a_i take three positive values $\gamma_1 < \gamma_2 < \gamma_3$. Then, $\mathcal{S} \subseteq \mathcal{R}_0 = [f_1, f_3]$. Three situations, shown on figures 9(*a*), (*b*) and (*c*) respectively, may happen:

(1) $\mathcal{R}_1 = \mathcal{R}_0$ then the support of $P(r)$ is $\mathcal{S} = \mathcal{R}_0$.

(2) $\mathcal{R}_1 \subset \mathcal{R}_0$ and the hole $\mathcal{H}_1 = \mathcal{R}_0 - \mathcal{R}_1$ is connected. Then, on one side (e.g. the right one on figure 9(*b*)) there exists an infinite number of pairwise disjoint images of $\mathcal{H}_1$ which are also excluded from the support; while on the other side the number of images of $\mathcal{H}_1$ is finite (possibly zero). Indeed, the lower ends of these images evolve by the mapping T_2 while the upper ends by T_1 (for the case of figure 9(*b*)). Since $f_1 < f_2$, these two ends must cross and the image of the hole disappears without descendent.

(3) $\mathcal{R}_1 \subset \mathcal{R}_0$ and the hole $\mathcal{H}_1 = \mathcal{R}_0 - \mathcal{R}_1$ is composed of two disconnected parts. Then in each of the three intervals which compose $\mathcal{R}_1$ there exists an infinite number of pairwise disjoint images of $\mathcal{H}_1$, and finally $\mathcal{S}$ is a Cantor set.

All the previous results are immediate consequences of the properties (i) and (ii) of T_a given in § 4.

5.3. The a_i take a continuous set of values

(i) We first consider the case where the a_i take their values γ in a continuous and connected set $\mathcal{A} = [\gamma_1, \gamma_2]$. Then one sees that in the three possible cases described on figures 3, 4 and 5, as γ continuously varies from γ_1 to γ_2, T_γ ($\mathcal{R}_0$) covers the whole $\mathcal{R}_0$. Therefore $\mathcal{R}_1 = \mathcal{R}_0$ and the support of $P(r)$ is $\mathcal{S} = \mathcal{R}_0$.

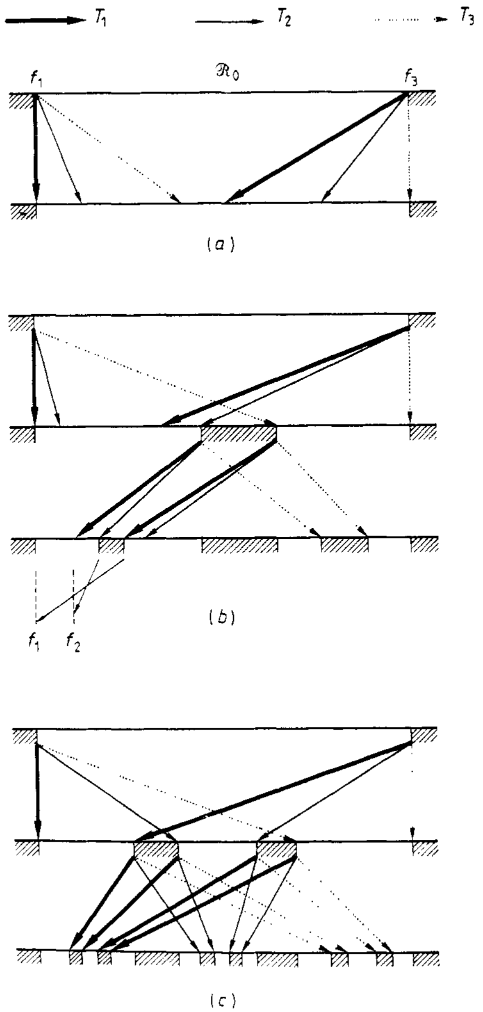

Figure 9. The mappings T_i and the first sets $\mathcal{R}_i$. The a_i take three positive values $\gamma_1 < \gamma_2 < \gamma_3$. In (*a*) the support of $P(r)$ is $\mathcal{R}_0$ with no hole. In (*b*) there is an infinite sequence of holes on the right of the initial hole and a finite sequence on its left. In (*c*) there are three infinite sequences of holes.

(ii) Let now $\mathcal{A}$ be the union of two disconnected continuous sets $[\gamma_1, \gamma_2]$ and $[\gamma_3, \gamma_4]$. We consider only the generic case when the a_i take positive values $(0 < \gamma_1 < \gamma_2 < \gamma_3 < \gamma_4)$. Then using the same arguments as before, one shows that there never exists an infinite number of holes in $\mathcal{R}_0$. Indeed, either $\mathcal{R}_1 = \bigcup_{\gamma \in \mathcal{A}} T_\gamma(\mathcal{R}_0) = \mathcal{R}_0$ as in figure 10(*a*) and then the support of $P(r)$ is $\mathcal{S} = \mathcal{R}_0$, or there exists a first hole $\mathcal{H}_1 = \mathcal{R}_0 - \mathcal{R}_1$ as in figure 10(*b*). But in this latter case, at the next step, either this hole has no descendent as shown on the right-hand side of figure 10(*b*), or there still exists a hole (left-hand side of figure 10(*b*)). But as in subsection 5.2 this hole must disappear since its lower ends evolve by T_2 while its upper ones by T_1, and $\gamma_1 < \gamma_2$.

5.4. The integrated distribution function F(r)

Clearly $F(r) = 0$ for $r < r_{\min}$ and $F(r) = 1$ for $r > r_{\max}$. Also $F(r)$ is constant in any interval in $\mathcal{R}_0$ not belonging to the support of $P(r)$, if such interval exists. The value of $F(r)$ at any of these flat portions can be determined from equation (3.9) if one knows how to characterise these flat portions. For simplicity the results are given only

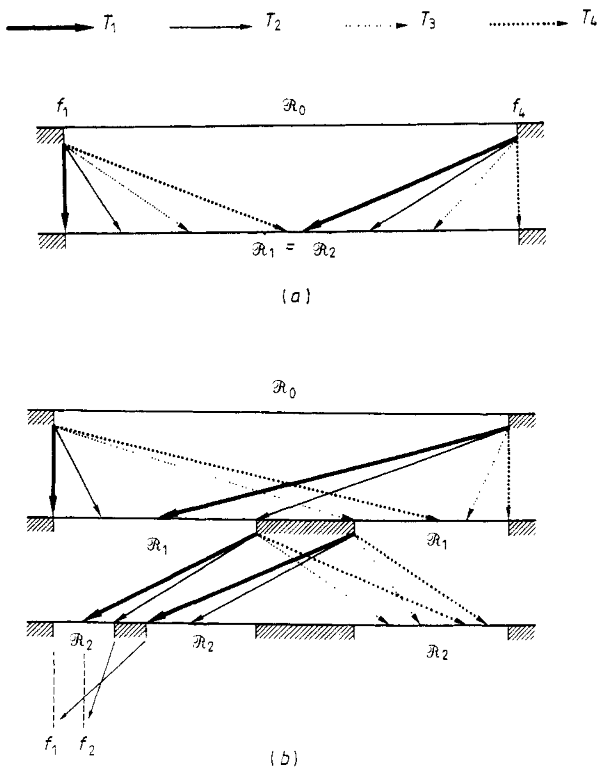

Figure 10. The mappings T_i and the first intervals $\mathcal{R}_i$. The a_i take values in two disconnected intervals $[\gamma_1, \gamma_2]$ and $[\gamma_3, \gamma_4]$ with $0<\gamma_1<\gamma_2<\gamma_3<\gamma_4$. In (*a*) the support of $P(r)$ is $\mathcal{R}_0$ with no hole. In (*b*) there is a finite sequence of holes in the left of the initial hole and no hole on its right.

for the cases studied in § 5.1, when the a_i take two values γ_1 and γ_2 with probabilities p_1 and p_2 respectively ($p_1+p_2=1$), with either $0\leq\gamma_1<\gamma_2$ or $\gamma_1<0\leq\gamma_2$. Then we assume that we are in the case when $\mathcal{R}_{i+1}\subset\mathcal{R}_i$ for all $i=0, 1, \ldots$; i.e. the support of $P(r)$ is a Cantor set.

Let us first consider the case when γ_1 and γ_2 are positive. Then, according to figure 3(*b*), $F(r)$ is constant in the interval $[\mathcal{H}_1]=[T_1(f_2), T_2(f_1)]$ where $T_i\equiv T_{\gamma_i}$, $i=1, 2$. It is also constant in any image of $[\mathcal{H}_1]$ by T_1 and T_2 any number of times and in any order, i.e. in the interval $[T_{\alpha_1}\ldots T_{\alpha_n}T_1(f_2), T_{\alpha_1}\ldots T_{\alpha_n}T_2(f_1)]$, where each $\alpha_j, j=1,\ldots,n$ is either γ_1 or γ_2. As T_1 maps $\mathcal{R}_0$ on $[f_1, T_1(f_2)]$ and this happens with probability p_1, one has $F(r)=p_1$ for r in $[\mathcal{H}_1]$. Since T_1 maps on the lower side and T_2 on the upper side, and these with probabilities p_1 and p_2 respectively, one sees that

$$\begin{aligned} F([T_1X, T_1Y]) &= p_1F([X, Y]), \\ 1-F([T_2X, T_2Y]) &= p_2\{1-F([X, Y])\}, \end{aligned} \tag{5.10}$$

where $[X, Y]$ is any of the flat portions mentioned above. Thereby we can determine the value of $F(r)$ for r belonging to any interval where $P(r)=0$. This kind of integrated probability distribution is referred as a devil's staircase, see figure 7(*b*).

Next, let the a_i take the two values $\gamma_1<0$ and $\gamma_2>0$. According to figure 4(*b*), $F(r)$ is constant in the interval $[\mathcal{H}_1]=[T_1(r_{\min}), T_2(r_{\min})]$, $r_{\min}=T_1(f_2)$. It is also constant on the images of $[\mathcal{H}_1]$, $[T_{\alpha_1}\ldots T_{\alpha_n}T_\alpha(r_{\min}), T_{\alpha_1}\ldots T_{\alpha_n}T_{\alpha'}(r_{\min})]$ where each α_j for $j=1,\ldots,n$ is either γ_1 or γ_2; either $\alpha=\gamma_1$ and $\alpha'=\gamma_2$ or $\alpha=\gamma_2$ and $\alpha'=\gamma_1$, and the number of γ_1 among $\alpha_1,\ldots,\alpha_n, \alpha'$ is even; including zero. Arguments similar to the above show that $F(r)=p_1$ for r in $[\mathscr{H}_1]$, and

$$\begin{aligned} F([T_1X, T_1Y]) &= p_1\{1-F([Y,X])\}, \\ 1-F([T_2X, T_2Y]) &= p_2\{1-F([X,Y])\}, \end{aligned} \tag{5.11}$$

where $[X, Y]$ is any of the above intervals in which $P(r)=0$. We can thus again compute the value of $F(r)$ for any interval not belonging to the support of $P(r)$.

6. Conclusion

Let us note that the shape of the probability distribution is partly independent of the explicit recurrence relation. Namely, any mapping $r_{n+1}=T_a(r_n)$ which is monotonous with respect to both r_n and a, yields the same kind of behaviour.

Since any point of the support $\mathscr{S}$ of the probability distribution $P(r)$ is associated with an infinite sequence of mappings, it can be viewed as the realisation of the corresponding pattern of the random parameters along the chain. If the parameters were not random, the support $\mathscr{S}$ would be reduced to a single point. Thus the effect of the disorder is to spread the probability distribution. The possible disconnected nature of the support of $P(r)$ is related to the disconnectedness of the support $\mathscr{A}$ of the probability distribution of the random parameters. In particular, a Cantor set may occur only if $\mathscr{A}$ consists of a finite number of points. The existence of holes reflects the fact that some values of the free energy cannot be reached; it is a blocking effect due to the discrete nature of the random variables.

The spreading of the probability distribution may be related to the existence of a large number of stable or metastable phases in the system (De Dominicis *et al* 1980, Parisi 1983).

Acknowledgments

We are thankful to J. des Cloizeaux for useful discussions, and to B Pidoux for his help with the numerical calculations.

Appendix 1. Determination of $\mathscr{R}_0$

We determine the minimum and the maximum values $r^{(n)}_{\min}$ and $r^{(n)}_{\max}$ of r after n iterations, and their limits $r_{\min}$ and $r_{\max}$ for large n. For brevity the point $T_{a_n}\ldots T_{a_1}(0)$ will be denoted by $(a_n, \ldots, a_1)$. Let us denote by α(resp $\bar\alpha$) the non-negative (resp. non-positive) values of a_i. The maximum and minimum values among the α(resp. $\bar\alpha$) are denoted by $\alpha_{\max}$ and $\alpha_{\min}$ (resp. $\bar\alpha_{\max}$ and $\bar\alpha_{\min}$):

$$-1\leqslant \bar\alpha_{\min}\leqslant \bar\alpha\leqslant \bar\alpha_{\max}\leqslant 0\leqslant \alpha_{\min}\leqslant \alpha\leqslant \alpha_{\min}\leqslant 1. \tag{A1.1}$$

One has to distinguish three cases.

(1) The a_i take only non-negative values. Starting from $r=0$, it follows from property (ii)(here and in what follows the properties (i), (ii) or (iii) refer to those given in § 4) of $T_a(r)$ that at the first step $r^{(1)}_{\min}=(\alpha_{\min})$ and $r^{(1)}_{\max}=(\alpha_{\max})$. Then, property (i) implies that at the second step the extreme values of r for a given $\alpha>0$ are $(\alpha\alpha_{\min})$

and $(\alpha\alpha_{\max})$ Now allowing α to vary and using the property (ii) one finds that $r_{\min}^{(2)}=(\alpha_{\min}\alpha_{\min})$ and $r_{\max}^{(2)}=(\alpha_{\max}\alpha_{\max})$. Repeating this argument one obtains from property (iii) in the limit

$$r_{\min}=f_{\alpha_{\min}}, \qquad r_{\max}=f_{\alpha_{\max}}. \tag{A1.2}$$

(2) The a_i take positive and negative values. From property (ii) one has $r_{\min}^{(1)}=(\bar{\alpha}_{\min})$ and $r_{\max}^{(1)}=(\alpha_{\max})$. In the second step one has to consider the sign of a_2. For a given $\alpha>0$ one gets at the second step the extreme values $(\alpha\bar{\alpha}_{\min})$ and $(\alpha\alpha_{\max})$. Varying $\alpha>0$ yields from property (ii) the least and the greatest values $(\alpha_{\min}\bar{\alpha}_{\min})$ and $(\alpha_{\max}\alpha_{\max})$. For $\bar{\alpha}<0$, $T_{\bar{\alpha}}$ is a decreasing function of r. Then one obtains the extreme values $(\bar{\alpha}_{\min}\alpha_{\max})$ and $(\bar{\alpha}_{\max}\bar{\alpha}_{\min})$. Now using property (ii) one has $(\bar{\alpha}_{\max}\bar{\alpha}_{\min})\leq(\alpha_{\min}\bar{\alpha}_{\min})$ and therefore $r_{\min}^{(2)}=(\bar{\alpha}_{\min}\alpha_{\max})$ and $r_{\max}^{(2)}=(\alpha_{\max}\alpha_{\max})$. Repeating the above argument one finds from property (iii) that

$$r_{\min}=T_{\bar{\alpha}_{\min}}(f_{\alpha_{\max}}), \qquad r_{\max}=f_{\alpha_{\max}}. \tag{A1.3}$$

(3) The a_i take only non-positive values. From property (ii), at the first step $r_{\min}^{(1)}=(\bar{\alpha}_{\min})$ and $r_{\max}^{(1)}=(\bar{\alpha}_{\max})$. For a given $\bar{\alpha}<0$, $T_{\bar{\alpha}}$ is a decreasing function of r, property (i); consequently at the second step the extreme values of r are $(\bar{\alpha}\bar{\alpha}_{\max})$ and $(\bar{\alpha}\bar{\alpha}_{\min})$. Allowing $\bar{\alpha}$ to vary and using property (ii) one gets $r_{\min}^{(2)}=(\bar{\alpha}_{\min}\bar{\alpha}_{\max})$ and $r_{\max}^{(2)}=(\bar{\alpha}_{\max}\bar{\alpha}_{\min})$. Repetition of this argument implies

$$r_{\min}^{(n+1)}=T_{\bar{\alpha}_{\min}}(r_{\max}^{(n)}), \qquad r_{\max}^{(n+1)}=T_{\bar{\alpha}_{\max}}(r_{\min}^{(n)}). \tag{A1.4}$$

Hence in the large n limit, $r_{\min}$ and $r_{\max}$ are the attractive fixed points of the homographic mappings $T_{\bar{\alpha}_{\min}}T_{\bar{\alpha}_{\max}}$ and $T_{\bar{\alpha}_{\max}}T_{\bar{\alpha}_{\min}}$ respectively.

The arguments developed above use the fact that the initial value of r is zero. Actually we could have started with any point on the real line and ended in the limit of a large number of iterations with the same domain $\mathscr{R}_0=[r_{\min}, r_{\max}]$†. This follows from the fact that in the iterative procedure a point r is either in $\mathscr{R}_0$ and from (4.8) all its images remain in $\mathscr{R}_0$, or it is in $\mathscr{D}_0$ and then the probability for all its successive images to remains in $\mathscr{D}_0$ vanishes in the limit of a large number of iterations. Indeed, taking into account the attractive character of the fixed points in terms of which $r_{\min}$ and $r_{\max}$ are expressed in table 3, one shows that for any r in $\mathscr{D}_0$ there exists an integer n and a set $\{a_1, \ldots, a_n\}$ such that $T_{a_n}\ldots T_{a_1}(r)$ belongs to $\mathscr{R}_0$. Then the probability p that at least one image of r after n steps of iterations belongs to $\mathscr{R}_0$ satisfies

$$p\geq\prod_{i=1}^{n}p(a_i)>0. \tag{A1.5}$$

Consequently, from the independence of the random variables a_i, the probability that all the images of r after nm iterations be outside $\mathscr{R}_0$ is $(1-p)^m$ which goes to zero as m tends to infinity.

Appendix 2. Proof of equations (4.11) and (4.12)

Since for all non-zero a, T_a maps $\mathbb{R}$ onto $\mathbb{R}$ (property (v) of § 4), for any $a\neq0$ and all r' there exists an $r(a)$ such that $r'=T_a[r(a)]$.

† J des Cloizeaux, private communication.

We first derive equation (4.11), namely we show that for all $i=0, 1, \ldots$ the two sets $\mathcal{R}_{i+1}=\mathbb{R}-\mathcal{D}_{i+1}$ and $\bigcup_{a\in\mathcal{A}} T_a(\mathcal{R}_i)$ are equal. Indeed, r' belongs to $\mathcal{R}_{i+1}$ iff it does not belong to $\mathcal{D}_{i+1}$, i.e. iff there exists an a in $\mathcal{A}$ such that $r(a)$ does not belong to $\mathcal{D}_i$ and thus belongs to $\mathcal{R}_i=\mathbb{R}-\mathcal{D}_i$. Finally r' belongs to $\mathcal{R}_{i+1}$ iff there exists an a in $\mathcal{A}$ such that $r(a)$ belongs to $\mathcal{R}_i$ and thus iff r' belongs to $\bigcup_{a\in\mathcal{A}} T_a(\mathcal{R}_i)$.

Let us now show by induction that the $\mathcal{R}_i$; $i=0, 1, \ldots$ form a sequence of nested intervals. It follows from (4.8) and (4.11) that $\mathcal{R}_1\subseteq\mathcal{R}_0$. Let us assume $\mathcal{R}_i\subseteq\mathcal{R}_{i-1}$. From (4.11), for all r' in $\mathcal{R}_{i+1}$ there exists an a in $\mathcal{A}$ and an r in $\mathcal{R}_i$ such that $r'=T_a(r)$. Now r in $\mathcal{R}_i$ is also in $\mathcal{R}_{i-1}$ from our inductive assumption; therefore $T_a(r)$ i.e. r' belongs to $\mathcal{R}_i$.

Appendix 3. About the existence of holes in $\mathcal{R}_0$

(i) $0<\gamma_1<\gamma_2$. A partial answer for the relative positions of $T_1(f_2)$ and $T_2(f_1)$ is as follows.

Since one has:

$$T_1(f_2)=(\gamma_1/\gamma_2)T_2(f_2)=(\gamma_1/\gamma_2)f_2, \tag{A3.1}$$

we consider the function $\varphi(\gamma)=f_\gamma/\gamma^2$, where f_γ is given by equation (4.1). The values of $\varphi(\gamma)$ are $+\infty$ and $b^{1/2}$ for $\gamma=+0$ and 1 respectively. The sign of its derivative $\varphi'(\gamma)$ is the same as the sign of $-3b-(2-\gamma)(1-2\gamma)/\gamma$. This factor vanishes at

$$\gamma=c\equiv\tfrac{1}{4}\{5-9b-3[(1-b)(1-9b)]^{1/2}\}. \tag{A3.2}$$

Therefore, $\varphi'(\gamma)<0$ either if $b\geqslant\frac{1}{9}$ or if $b<\frac{1}{9}$ and $\gamma_2\leqslant c$, and that $\varphi'(\gamma)>0$ if $b<\frac{1}{9}$ and $c\leqslant\gamma_1$. One thereby finds that:

If $\frac{1}{9}\leqslant b\leqslant 1$ all $0<\gamma_1<\gamma_2$, or if $b<\frac{1}{9}$ and $0<\gamma_1<\gamma_2\leqslant c$, then $T_1(f_2)<T_2(f_1)$ and there are holes in $\mathcal{R}_0$.

If $b<\frac{1}{9}$ and $c\leqslant\gamma_1<\gamma_2$ then $T_1(f_2)\geqslant T_2(f_1)$ and there are no holes in $\mathcal{R}_0$.

If $b<\frac{1}{9}$ and $0<\gamma_1<c<\gamma_2$ the situation is more delicate.

(ii) $\gamma_1<0<\gamma_2$. About the relative position of $T_1T_1(f_2)$ and $T_2T_1(f_2)$ the result is

$$T_1T_1(f_2)<T_2T_1(f_2)\Longleftrightarrow 1-b\gamma_2/\gamma_1>\gamma_2-\gamma_1. \tag{A3.3}$$

One should note that this condition is especially satisfied for all γ_2 if $\gamma_1+b\geqslant 0$. These results follow from the fact that the first inequality of (A3.3) is equivalent to $T_2T_1(f_2)>0$. Note that in the special case $-\gamma_1=\gamma_2=\gamma>0$ there exist holes in $\mathcal{R}_0$ iff (see figure 6).

$$1+b>2\gamma. \tag{A3.4}$$

References

Brandt U and Gross W 1978 *Z. Phys.* B **31** 237
Bruinsma R and Aeppli G 1983 *Phys. Rev. Lett.* **50** 1494
De Dominicis C 1978 *Phys. Rev.* B **18** 4913
—— 1979 *C.R. Acad. Sci., Paris* B **289** 281
De Dominicis C, Gabay M, Garel T and Orland H 1980 *J. Physique* **41** 923

Derrida B, Vannimenus J and Pomeau Y 1978 *J. Phys. C: Solid State Phys.* **11** 4749
Dyson F J 1953 *Phys. Rev.* **92** 1331
Edwards S F and Anderson P W 1975 *J. Phys. F: Met. Phys.* **5** 985
Fan C and McCoy B M 1969 *Phys. Rev.* **182** 614
Furstenberg H 1963 *Trans. Am. Math. Soc.* **108** 377
Györgyi G and Rujan P 1984 *Eötvös University Budapest, Hungary preprint*
Hausdorff F 1957 *Set Theory* (*New York: Chelsea Publishing Co*)
Maillard J M 1978 *Thèse de 3e cycle, Université Pierre et Marie Curie Paris*
Parisi G 1983 *Phys. Rev. Lett.* **50** 1946